

Linear Viscoelastic Behavior of Compatibilized PMMA/PP Blends

Adriana Martinelli Catelli de Souza,* Patrícia Schmid Calvão,* Nicole Raymonde Demarquette[†]

Metallurgical and Materials Engineering Department, Escola Politécnica, Universidade de São Paulo, Av. Professor Mello Moraes, 2463 CEP 05508-900 São Paulo, SP, Brazil

*Present Address: Materials Engineering Department, Centro Universitário da FEI, Av. Humberto de Alencar Castelo Branco, 3972 CEP 09850-901 São Bernardo do Campo, SP, Brazil

[†]Present Address: Département de Génie Mécanique, Ecole de Technologie Supérieure, 1100 Notre-Dame Ouest, H3C 1K3 Montreal, Canada

Correspondence to: N. R. Demarquette (E-mail: nicoler.demarquette@etsmtl.ca)

ABSTRACT: In this work, the morphology and linear viscoelastic behavior of PMMA/PP blends to which a graft copolymer PP-g-PMMA has been added was studied. The copolymer concentration varied from 1 to 10 wt % relative to the dispersed phase concentration. The rheological data were used to infer the interfacial tension between the blended components. It was observed that PP-g-PMMA was effective as a compatibilizer for PMMA/PP blends. For PP-g-PMMA concentration added below the critical concentration of interface saturation, two rheological behaviors were observed depending on the blend concentration: for 70/30 blend, the storage modulus, at low frequencies, increased as compared to the one of the unmodified blend; for 90/10 blend, it decreased. For 90/10 blend, the relaxation spectrum presented an interfacial relaxation time related to the presence of the compatibilizer (τ_β). For PP-g-PMMA concentrations added above the critical concentration of interface saturation, the storage modulus of all blends increased as compared with the one of the unmodified blend. © 2012 Wiley Periodicals, Inc. *J. Appl. Polym. Sci.* 129: 1280–1289, 2013

KEYWORDS: blends; compatibilization; rheology; viscosity; viscoelasticity

Received 29 June 2012; accepted 31 October 2012; published online 3 December 2012

DOI: 10.1002/app.38809

INTRODUCTION

Due to their ability to combine the properties of their components in a unique product, polymer blending have proven to be one of the most efficient way to satisfy new requirements for materials properties.¹ The great majority of commercial polymers are immiscible forming multiphase materials. The properties of the resultant blends depend strongly on their morphology, which can be controlled through compatibilizer addition. These compatibilizers can be premade copolymers having block miscible with both components of the blends (physical compatibilization) or can be formed in situ by reactive processing (chemical compatibilization). Due to their ability to accumulate on the interface between the blended components, the compatibilizer addition results in a reduction of the dispersed phase size,^{2–4} stabilization of morphology inhibiting dispersed phase coalescence,⁵ decrease of interfacial tension between the blends components,^{3,6,7} besides an improvement of the blend properties that is a direct consequence of the change of morphology.⁸

Rheology can be a nice tool to characterize the morphology of polymer blends and its evolution. In particular, the characterization of polymer blends in the viscoelastic regime enables the

quantification of their morphology as well as of the interfacial tension between the blended components: when submitted to small amplitude oscillatory shear, immiscible binary blends show an increase of elasticity at low frequencies, which can result in the presence of a secondary plateau in the curve of the storage modulus. That plateau, that can be associated to a relaxation time, τ_β , is due to the relaxation of the shape of the dispersed phase of the blend when the blend is sheared.⁹ In the case of compatibilized blends, the increase of elasticity is normally larger and an additional relaxation time, τ_β , which can be attributed to the action of the compatibilizer at the blend interface may be observed. That interfacial relaxation time (τ_β), that has been observed for compatibilized blends through the addition of premade block,¹⁰ graft,^{11,12} or random copolymers¹³ or modifying chemically one of the polymers of the blends,¹⁴ can be attributed to the relaxation of Marangoni stresses tangential to the interface between the dispersed and matrix phases.^{15–22} These Marangoni stresses are induced by the presence of a gradient of compatibilizer concentration at the interface which results in a gradient of interfacial tension.^{19,20} That interfacial relaxation time (τ_β) was shown to be dependent on the morphology and rheological properties of the blends, surface

Table I. The Most Important Constitutive Models Developed that Provide an Analytical Expression for the Complex Modulus

Model	Considerations	Constitutive equations
Generalized Palierne ^{27,28}	Non diluted viscoelastic suspensions	$G^*(\omega) = G_m^*(\omega) \left[\frac{1 + 3/2 \sum_i \frac{\Phi_i E_i^*}{D_i}}{1 - \sum_i \frac{\Phi_i E_i^*}{D_i}} \right] \quad (1)$
	Where	$E_i = 2(G_d^* - G_m^*)(19G_d^* + 16G_m^*) + \frac{48\beta_d^* \Gamma}{R_i^2} + \frac{32\beta_s^* (\Gamma + \beta_d^*)}{R_i} + \frac{8\Gamma}{R_i} (5G_d^* + 2G_m^*) + \frac{2\beta_d^*}{R_i} (23G_d^* - 16G_m^*) + \frac{4\beta_s^*}{R_i} (13G_d^* + 8G_m^*) \quad (2)$
	And	$D_i = (2G_d^* + 3G_m^*)(19G_d^* + 16G_m^*) + \frac{48\beta_d^* \Gamma}{R_i^2} + \frac{32\beta_s^* (\Gamma + \beta_d^*)}{R_i} + \frac{40\Gamma}{R_i} (G_d^* + G_m^*) + \frac{2\beta_d^*}{R_i} (23G_d^* + 32G_m^*) + \frac{4\beta_s^*}{R_i} (13G_d^* + 12G_m^*) \quad (3)$
		<p>*To simplify the equation the (ω) have been omitted in eqs. (2) and (3). However one should read $G_j^*(\omega)$, instead of G_j^* (where $j = d$ or m) and $\beta_k^*(\omega)$ instead of β_k^* (where $k = s$ or d).</p> <p>where i refers to the ith particle fraction, that is, R_i is the radius of the ith particle fraction, $G^*(\omega)$, $G_m^*(\omega)$, $G_d^*(\omega)$ are the complex shear moduli of the blend, matrix, and dispersed phase, $\beta_d^*(\omega)$: the surface dilatation modulus, $\beta_s^*(\omega)$ the surface shear modulus, and Γ is the interfacial tension.</p>
Simplified Palierne ⁹	(1) $\beta_d^*(\omega)$, $\beta_s^*(\omega)$ are set equal to zero (in the case of uncompatibilized blends)	$G^* = G_m^* \frac{40 \left(\frac{\Gamma}{R_i} \right) [G_m^* + G_d^*] + [2G_d^* + 3G_m^*] [16G_m^* + 19G_d^*] + 3\Phi_i \left[4 \left(\frac{\Gamma}{R_i} \right) [2G_m^* + 5G_d^*] + [G_d^* - G_m^*] [16G_m^* + 19G_d^*] \right]}{40 \left(\frac{\Gamma}{R_i} \right) [G_m^* + G_d^*] + [2G_d^* + 3G_m^*] [16G_m^* + 19G_d^*] + 2\Phi_i \left[4 \left(\frac{\Gamma}{R_i} \right) [2G_m^* + 5G_d^*] + [G_d^* - G_m^*] [16G_m^* + 19G_d^*] \right]} \quad (4)$
	(2) Morphology should be uniform, that is, $R_i/R_n < 2.3$	<p>*To simplify the equation the (ω) have been omitted in eq. (4).</p> <p>where $G^*(\omega)$, $G_m^*(\omega)$, $G_d^*(\omega)$ are the complex shear moduli of the blend, matrix and dispersed phase, respectively; Γ is the interfacial tension between the components of the blend; Φ_i is the volume fraction of dispersed phase and R_i is the volume average radius.</p>
Bousmina ²⁹	Takes into account the circulation of the fluid inside the dispersed phase drop	$G^*(\omega) = G_m^*(\omega) \frac{2 \left(G_d^*(\omega) + \frac{\Gamma}{R_i} \right) + 3\Phi \left(G_d^*(\omega) + \frac{\Gamma}{R_i} - G_m^*(\omega) \right)}{2 \left(G_d^*(\omega) + \frac{\Gamma}{R_i} \right) + 3G_m^*(\omega) - 2\Phi \left(G_d^*(\omega) + \frac{\Gamma}{R_i} - G_m^*(\omega) \right)} \quad (5)$
		<p>where $G^*(\omega)$, $G_m^*(\omega)$, $G_d^*(\omega)$ are the complex shear moduli of the blend, matrix and dispersed phase, respectively; Γ is the interfacial tension between the components of the blend; Φ is the volume fraction of dispersed phase and R_i is the volume average radius.</p>

Table II. Model Based on the Analysis of the Relaxation Spectrum of the Blends

Model	Considerations	Constitutive equations
Jacobs et al. ³⁰	(1) Both polymers are considered Newtonian fluids.	$\tau_F = \frac{\tau_{12}}{2} \left[1 - \left(1 - 4 \frac{\tau_{11}}{\tau_{12}} \right)^{0.5} \right] \quad (6)$ $\tau_\beta = \frac{\tau_{12}}{2} \left[1 + \left(1 - 4 \frac{\tau_{11}}{\tau_{12}} \right)^{0.5} \right] \quad (7)$
	(2) $\beta_d^*(\omega)$ and $\beta_s^*(\omega)$ are considered purely elastic (can be set equal to a constant called β_{10} and β_{20} , independent of frequency).	with
		$\tau_{11} = \frac{R_v \eta_m}{4\Gamma} \frac{(19K + 16)[2K + 3 - 2\Phi(K - 1)]}{10(K + 1) + \frac{\beta_{20}}{\Gamma}(13K + 12) - 2\Phi\left((5K + 2) + \frac{\beta_{20}}{2\Gamma}(13K + 8)\right)} \quad (8)$
	(3) Only one of the two parameters β_{10} or β_{20} is set different from zero as their role can be easily exchanged	and
		$\tau_{12} = \frac{R_v \eta_m}{8\beta_{20}} \frac{10(K + 1) + \frac{\beta_{20}}{\Gamma}(13K + 12) - 2\Phi\left((5K + 2) + \frac{\beta_{20}}{2\Gamma}(13K + 8)\right)}{(1 - \Phi)} \quad (9)$
		where R_v is volume average radius, η_m is the viscosity of the matrix, Φ is volume fraction of dispersed phase, K is viscosity ratio, and Γ is interfacial tension.

coverage, interfacial tension gradient,^{21,22} copolymer concentration,^{13,21,22} and copolymer molar mass.¹²

The extent to which the addition of compatibilizers affects the rheological behavior, that is, the deformation/relaxation behavior of the dispersed phase droplets during flow, was shown to depend on the concentration added. As mentioned above, when a compatibilized blend is sheared, a gradient of compatibilizer concentration may be generated at the matrix/dispersed phase interface. It was observed that for blends containing compatibilizer concentration below the critical concentration of interface saturation (C_∞), the compatibilizer moved from the droplet equator to the poles resulting in tip streaming phenomena.^{23–26}

When the hydrodynamic stress is removed, the Marangoni stresses promoted a faster relaxation of the dispersed phase droplets compared with the ones of the blend without compatibilizer addition. However, for blends containing compatibilizer concentration above the critical concentration of interface saturation (C_∞), the dispersed phase droplet surface is totally recovered by compatibilizer; local entanglements are generated at the interface and the Marangoni stresses act inhibiting the dispersed phase droplets deformation. Consequently, when the hydrodynamic stress is removed, the dispersed phase droplets relax slower.

For the last 20 years, several emulsion models were developed to relate the linear viscoelastic response of polymer blends to their

morphology, composition, and interfacial tension between the components. Tables I and II summarize the most important constitutive models developed. Table I presents the models that provide an analytical expression for the complex modulus: in this case if the morphology is quantified, the best fit of eqs. (1) or (4) or (5) to experimental data of complex modulus of the blend leads to the value of interfacial tension between the components of the blend. Two main models were developed: Palierne's^{27,28} and Bousmina's²⁹ models. Palierne considered nondiluted viscoelastic suspensions and developed a constitutive equation that predicts the behavior of compatibilized blends (Generalized Model)^{27,28} or not (Simplified Model).⁹ Later, Bousmina developed another constitutive equation, which can be used for both compatibilized and noncompatibilized blends.²⁹ The principal difference between Palierne's and Bousmina's models, relies on the treatment given to the interface. Bousmina's model is more adequate than Palierne's model for fluids with internal structures such as LCP; however, both models are quantitatively very similar. Table II presents Jacob's et al. model that is based on the analysis of the relaxation spectrum of the blends and provide analytical expressions for the relaxation times of the dispersed phase (τ_f) and the one observed in compatibilized blends (τ_β).³⁰

In this work, the linear viscoelastic behavior of PMMA/PP (70/30 and 90/10) blends to which a graft copolymer PP-g-PMMA

Table III. Materials Used in This Work

Polymer/Copolymer	M_w	M_n	M_w/M_n	η_o (Pa.s) at 200°C	PP/MMA (%)
PMMA	65,000	31,000	2.1	24,000	-
PP	340,000	75,000	4.5	3,700	-
PP-g-PMMA	-	-	-	-	50/50

was added at concentrations above and below the critical concentration of interface saturation was studied. The rheological behavior of these blends was compared to Palierne's and Bousmina's models and the relaxation spectra of the blends were inferred and analyzed using the Jacob's equations.

EXPERIMENTAL

Materials

Commercial PMMA from Metacril (Brazil) and polypropylene (PP) from Quattor S. A. (Brazil) were used in this work. Graft copolymer PP-g-PMMA from Lyondell-Basell (USA) was used as compatibilizer. The properties of the polymers and compatibilizer are listed in Table III.

Experimental Procedures

The PMMA/PP blends were obtained in a 90/10 and 70/30 weight compositions. The PP-g-PMMA concentration varied from 0 to 10 wt % with respect to the dispersed phase PP. The PMMA/PP blends were prepared by melt blending in a Haake PolyLab 900/Rheomix 600 p batch mixer (Haake – Germany) at 200°C using a rotor speed of 50 rpm for 12 min. The compatibilizer (PP-g-PMMA) was first mixed with the minor phase (PP) and then blended to the matrix (PMMA). In the case of the unmodified blends, the minor phase was processed twice in order to have undergone the same thermomechanical history.

Samples for rheological and morphological analysis were obtained by compression molding. Discs of 25 mm diameter and 1 mm thickness were molded at a temperature of 200°C, under isostatic pressure for 10 min. The specimens were cooled in water at about 25°C.

Dynamic Frequency Sweep Tests were performed using a controlled stress rheometer SR5000 (TA Instruments, USA) under dry nitrogen atmosphere at 200°C. A plate-plate configuration was used with a gap size of 0.9 mm and a plate diameter of 25 mm. The measurements were carried out in the linear viscoelastic regime decreasing the frequency from 100 to 0.01 rad/s. Before the experiments, the specimens were dried at 70°C for 24 h in a vacuum oven at ~10 mbar.

The blends morphologies were characterized by scanning electron microscopy (SEM) using a Philips model XL 30 microscope (Philips, Netherlands). The samples were fractured in liquid nitrogen. Then, the samples were covered with gold using a Balzers sputter coater (model SCD-050; Balzers, Liechtenstein). Quantitative analysis of the morphology was performed using appropriate software (KS-300). The average radii of the dispersed phase (R_v and R_n) were calculated after analysis of the SEM photomicrographs. About 1000 particles were considered to calculate these parameters. For the calculation of the

average size of the dispersed phase, Saltikov's correction was used.³¹

RESULTS

Morphology

All blends studied in this work, compatibilized or not, presented a droplet dispersion morphology. Figure 1(a) shows the morphology of unmodified PMMA/PP (90/10) blend and Figure 1(b) shows the morphology of the respective blend modified with 10 wt % of PP-g-PMMA. Table IV presents the quantification of the morphology for the different blends studied here. It can be seen that the PP-g-PMMA addition results in a

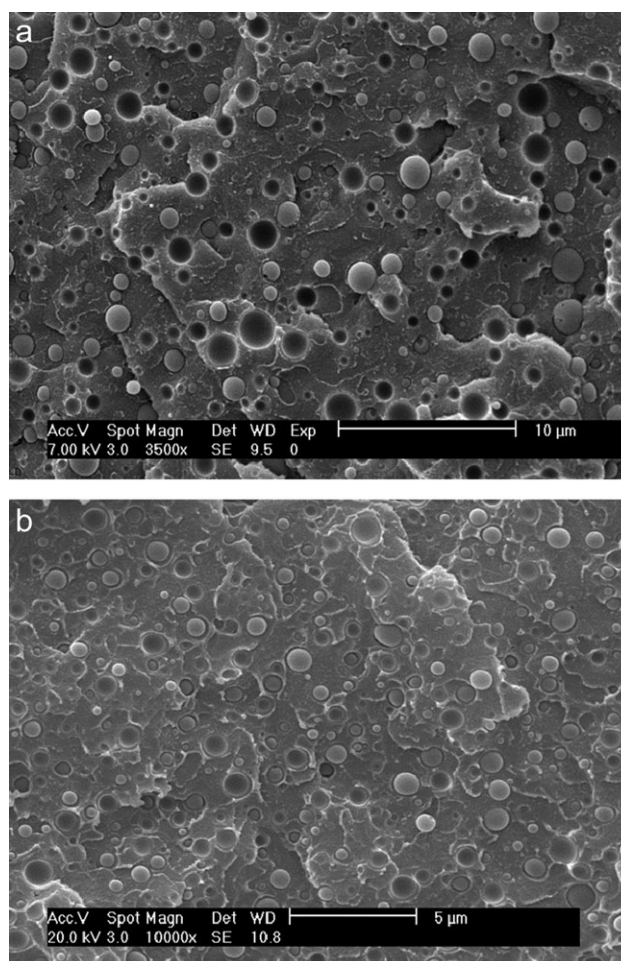


Figure 1. Morphology of PMMA/PP blends after compression molding: (a) unmodified PMMA/PP (90/10) blend; (b) PMMA/PP (90/10) blend modified with 10 wt % PP-g-PMMA.

Table IV. Quantification of the Morphology for the Different PMMA/PP Blends

Blend composition	PP-g-PMMA concentration (wt %) ^a	R_v (μm)	R_v/R_n
70/30	0	2.90	3.15
	1	2.40	3.24
	5	1.90	3.28
	10	1.70	3.27
90/10	0	0.84	3.00
	1	0.70	2.92
	10	0.51	2.21

^aWith respect to the dispersed phase PP.

decrease of the dispersed phase diameter for both modified blends.

Rheological Characterization

Before Dynamic Frequency Sweep Tests had been conducted, Time Sweep Tests for both PP and PMMA samples were

performed at 200°C for 5400 s (duration time of Dynamic Frequency Sweep Tests). It was observed that the complex viscosity of both polymers was stable during test, indicating thermal stability during Dynamic Frequency Sweep Tests. Figures 2(a,b) show the storage modulus at 200°C of PMMA/PP (70/30) and (90/10) blends, respectively, to which PP-g-PMMA has been added in different concentrations. The storage modulus at 200°C of PMMA and PP pure phases is also shown in Figure 2(a). The region for low frequencies is enlarged for a better visualization of the data. It can be seen that the PMMA/PP (90/10) blends show an increase of elasticity with increasing compatibilizer concentration when compared with the blends without PP-g-PMMA addition. This increase of elasticity has already been observed by several researchers.^{10,13,15–22,30} The PMMA/PP (70/30) blends present a different behavior: for compatibilizer concentrations above 5 wt %, an increase of elasticity with increasing compatibilizer concentration is observed while for compatibilizer concentration of 1 wt %, the blend shows a slight decrease of storage modulus when compared with the storage modulus of the unmodified PMMA/PP blend. Similar behavior has already been observed by other researchers in the case of PP/EVOH (90/10) blends to which a random ethylene/

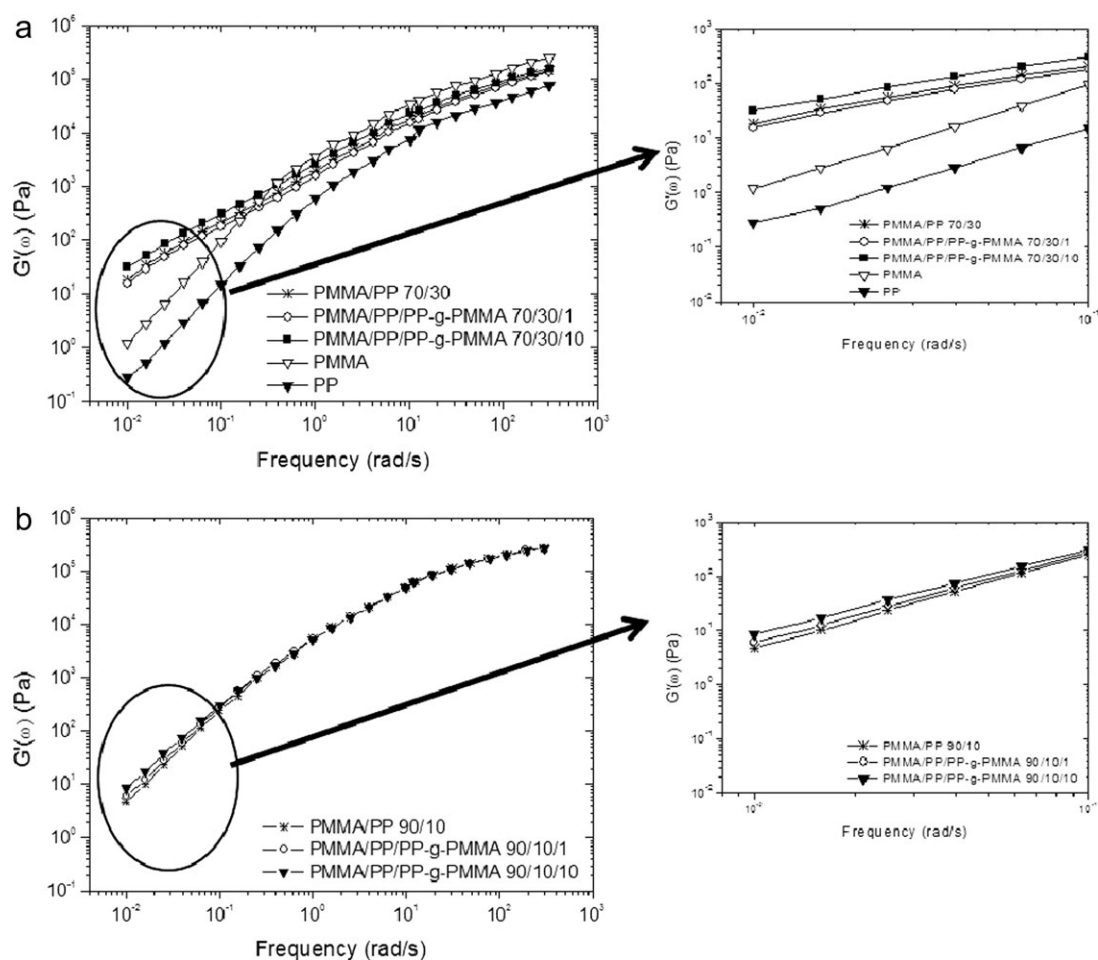


Figure 2. Storage modulus at 200°C of PMMA and PP pure phases and PMMA/PP (70/30) (a) and (90/10) (b) blends to which PP-g-PMMA has been added in different concentrations. The curves for both pure phases (PP and PMMA) were not added to Figure 2(b) for the sake of safety of clarity of the Figure.

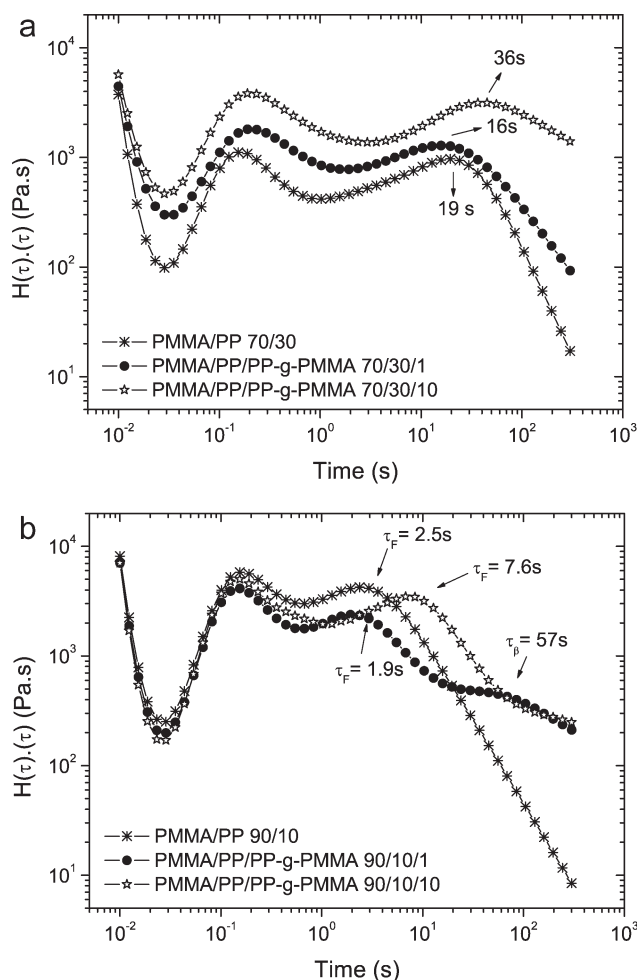


Figure 3. Relaxation spectra of PMMA/PP (70/30) (a) and (90/10) (b) blends compatibilized or not with PP-g-PMMA in different concentrations.

methacrylic acid copolymer partially neutralized with sodium³² was added and in the case of PE/PB (80/20) blends to which SBS was added.³³

To visualize better the relaxation phenomena observed in the rheological dynamic moduli, the relaxation spectra of the different blends studied in this work were calculated using the dynamic moduli data. The relaxation spectra were calculated using Honerkamp and Weese method.³⁴ Figure 3(a,b) show the relaxation spectra of PMMA/PP (70/30) and (90/10) blends, respectively, compatibilized or not with PP-g-PMMA. Only two concentrations of compatibilizer are shown for the sake of clarity of the Figures. It can be seen that PMMA/PP (70/30) blends compatibilized or not, present two relaxation times: one that could correspond to the superposition of relaxation of two phases of the blend and a second one that could correspond to the relaxation of the shape of the dispersed phase (τ_f). Similar behavior can be observed for the PMMA/PP (90/10) blend to which 10 wt % PP-g-PMMA was added. In the case of PMMA/PP (90/10) blend to which 1 wt % PP-g-PMMA was added, an additional relaxation time (τ_β), which could be related to the

relaxation of the interface induced by the presence of a compatibilizer concentration gradient is observed. Table V presents the values of the relaxation times obtained analyzing the relaxation spectra of the different blends studied in this work. The values of (τ_f) for PMMA/PP (70/30) and (90/10) blends to which PP-g-PMMA has been added in a concentration of 1 wt % are smaller than the ones of the unmodified blend whereas the values of (τ_f) for PMMA/PP (70/30) and (90/10) blends to which concentrations larger than 1 wt % of PP-g-PMMA was added are larger than the ones of the unmodified blend. Details will be discussed later.

Interfacial Tension

The experimental rheological data of PMMA/PP (70/30) and (90/10) blends compatibilized or not with PP-g-PMMA were fit to Bousmina's model to obtain the values of interfacial tension between PMMA and PP. Bousmina's model did not fit the experimental data for any value of interfacial tension tested for PMMA/PP (70/30) blend, making it impossible to obtain the interfacial tension using the blend in this composition (70/30). This behavior could be due to dispersed phase coalescence phenomenon during dynamic tests for PMMA/PP (70/30) blends. In a previous work, PMMA/PP (70/30) and (85/15) blends samples were frozen *in situ* in the rheometer to visualize and quantify morphology just after the Dynamic Frequency Sweep Tests.³⁵ The results indicated that coalescence did not occur for the PMMA/PP (85/15) blend during dynamic experiments. In the case of PMMA/PP (70/30) blend, coalescence occurred but did not upon addition of compatibilizer above 1 wt % (unpublished results). In the case of the PMMA/PP (90/10) blends compatibilized or not, Bousmina's model fitted perfectly to the experimental data. The values of interfacial tension that resulted in the best fit between experimental data and Bousmina's model are shown in Table V. The interfacial tension between PMMA and PP obtained is in good agreement with the value from literature.³⁶

As expected, the interfacial tension between PMMA and PP decreases with increasing PP-g-PMMA concentration indicating that this copolymer is effective as a compatibilizer for these blends.

The rheological data of PMMA/PP (70/30) and (90/10) blends compatibilized with PP-g-PMMA were also fit to the generalized Palierne's model to obtain the values of β_{20} in the case of compatibilized blends. The generalized Palierne's model did not fit the experimental data of PMMA/PP (70/30) blends compatibilized or not for any values of interfacial tension tested. However, the model fitted perfectly the experimental data of PMMA/PP (90/10) blends compatibilized or not as can be seen in Figure 4. This Figure shows a typical comparison between the experimental data and the predictions of Palierne's generalized model, using different values of β_{20} and the value of interfacial tension obtained by Bousmina's model. In this case, it is shown the rheological behavior of the 90/10 blend to which 10 wt % of PP-g-PMMA has been added. It can be seen that when a nonzero value of β_{20} is considered the quality of the fit increases considerably. Similar behavior has been shown by Asthana and Jayaraman³⁷ and Yee et al.¹³ The values of β_{20}

Table V. Relaxation Times Obtained Analyzing the Relaxation Spectra of the Different Blends Studied; Interfacial Tension Values Resulted in the Best Fit Between Experimental Data and Bousmina's Model; β_{20} Values Obtained Fitting Generalized Palierne Model to Experimental Data

Blend composition	PP-g-PMMA concentration (wt %)	Interfacial Tension (γ) (mN/m) obtained fitting Bousmina's Model to experimental data	Experimental data		Generalized Palierne Model	
			τ_f (s) Obtained by relaxation spectrum	τ_β (s) Obtained by relaxation spectrum	β_{20} (mN/m) Obtained using Jacobs equations	Estimated β_{20} (mN/m) Obtained fitting the experimental data to Palierne Model ^a
70/30	0	Not possible	19	-	-	-
	1	Not possible	16	-	-	Not possible
	5	Not possible	25	-	-	Not possible
	10	Not possible	36	-	-	Not possible
90/10	0	7	2.5	-	-	-
	1	6.5	1.9	57	0.45	0.43
	10	2.5	7.6	-	-	0.50

^aUsing Interfacial Tension values obtained by Bousmina's model.

corresponding to the best fit between experimental data and the Palierne's model are shown in Table V. It can be seen from Table V that when the concentration of PP-g-PMMA copolymer increases, β_{20} increases. Similar behavior has been seen by Riemann et al.,¹⁵ Jacobs et al.,³⁰ Van Hemelrijck et al.,²¹ Friederich and Antonov,¹² and Yee et al.¹³ Such a behavior was explained by the highest resistance of the compatibilizer layer at the interface to shear deformation.

DISCUSSION

Relaxation Spectrum

To identify the physical signification of the relaxation times found in the analysis of the relaxation spectra, their values were compared with predictions using Jacobs et al. model.³⁰ Figure 5(a,b) present (τ_f) and (τ_β) values, respectively, estimated using eqs. (6)–(9) as a function of β_{20} , for PMMA/PP (90/10) and (70/30) blends to which PP-g-PMMA has been added in concentrations of 1 and 10 wt % (only two concentrations of compatibilizer are shown for the sake of clarity of the Figures). In these estimations, the dispersed phase radius was taken from Table IV, the zero-shear viscosities of the individual phases were determined using the rheological data fitted to Carreau's model,³⁸ the interfacial tension was taken as the one which corresponded to the best fit of the experimental data to Bousmina's model using PMMA/PP (90/10) data and β_{20} is varied from 0.01 to 1 mN/m, which corresponded to values of β_{20} that were obtained in the literature for different compatibilized blends.^{13–16,18,20–22,30,37,39} The horizontal lines correspond to the relaxation time values found experimentally. It can be seen from Figure 5(a) that (τ_f) depends on the blend and compatibilizer concentration but that its dependence on β_{20} is relatively small. Assuming a relative error for the determination of R_v of 10%, for the determination of (τ_f) and (τ_β) of 15% and for the determination of zero shear viscosity of 3%, it can also be seen that the values estimated correspond to the values of the second relaxation time obtained in the analysis of Figure 3(a,b) independently of the value of β_{20} . Figure 5(b) shows that (τ_β)

decreases with increasing β_{20} and increases with increasing dispersed phase concentration. It can be also seen that the estimated value of (τ_β) for the PMMA/PP 90/10 blend to which 1 wt % graft copolymer was added, corresponds to the experimental value of the third relaxation time for a β_{20} value of around 0.45 mN/m indicating that in the case of PMMA/PP (90/10) blend to which 1 wt % of PP-g-PMMA was added it was possible to visualize the relaxation of the Marangoni stresses induced by the presence of the compatibilizer. For PMMA/PP 90/10 blend to which PP-g-PMMA has been added in a concentration of 10 wt %, the estimated value of (τ_β) decreases with increasing PP-g-PMMA concentration but could not be observed experimentally. It is therefore possible that for this PP-g-PMMA concentration, (τ_β) be superposed to (τ_f) as has been observed by other researchers when the compatibilizer concentration is high.^{12,17,20}

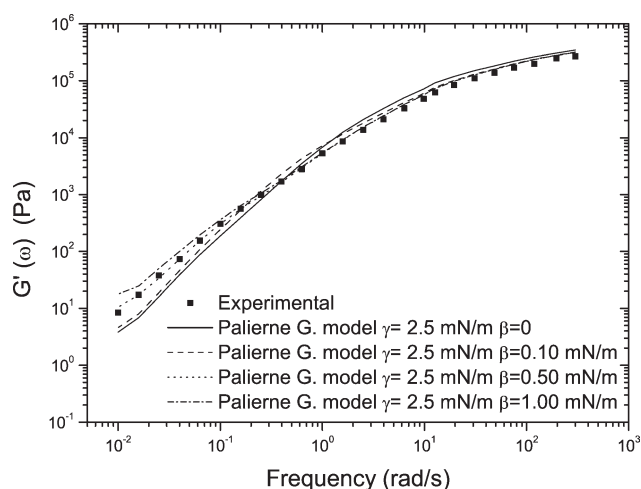


Figure 4. Comparison between the experimental data of PMMA/PP/PP-g-PMMA (90/10/10) and Generalized Palierne Model using different values of beta and the value of interfacial tension obtained by Bousmina's model.

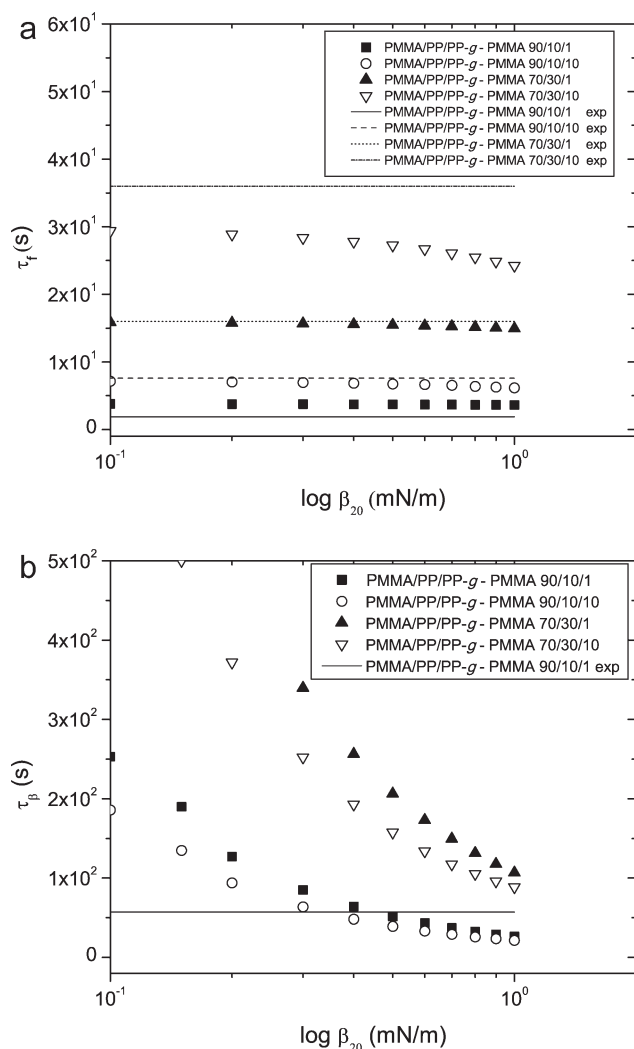


Figure 5. τ_f values as a function of β_{20} estimated using eqs. (6)–(9), for PMMA/PP (90/10), and (70/30) blends to which PP-g-PMMA has been added in concentrations of 1 and 10 wt % (a). τ_β values as a function of β_{20} estimated using eqs. (6)–(9), for PMMA/PP (90/10) and (70/30) blends to which PP-g-PMMA has been added in concentrations of 1 and 10 wt % (b).

For PMMA/PP 70/30 blend to which PP-g-PMMA has been added, the estimated values of (τ_β) is greater than 100 s [see Figure 5(b)] and therefore, should they physically exist, could not be observed experimentally. The visualization of relaxation times larger than 100 s requires performing dynamic experiments at frequencies lower than 0.002 rad/s.⁴⁰ To reach those frequencies, tests of a duration larger than 8 h would need to be performed and thermal degradation of the samples could occur. Besides, the moduli magnitude at these frequencies would be below the limit of resolution of the rheometer transducer. Only time temperature superposition (TTS) or use of creep measurements would allow reaching these frequencies but the use of TTS for blends is not always possible⁴¹ and creep experiments in blends are not always reproducible.^{42,43}

For concentrations of PP-g-PMMA larger than 1 wt %, the values of (τ_f) for PMMA/PP (70/30) and (90/10) blends are larger

than the ones of the unmodified blend, indicating that the relaxation of the shape of the dispersed phase droplets (τ_f) of these blends is slower than in the case of the unmodified blend. Such a behavior confirms the storage modulus data obtained for which an increase of elasticity was observed. However, the values of (τ_f) for PMMA/PP (70/30) and (90/10) blends to which PP-g-PMMA has been added in a concentration of 1 wt % are smaller than the ones of the unmodified blend, indicating that the relaxation of the shape of the dispersed phase droplets is faster than for the unmodified blend. In the case of 70/30 blend, this faster relaxation explains the smaller value of relaxation modulus observed at low frequencies. The higher value of relaxation modulus observed for 90/10 blends to which 1 wt % PP-g-PMMA has been added, originates from the presence of the relaxation of Marangoni stresses (with a relaxation time τ_β). Similar behavior has already been observed by Rieman et al.^{15,16} and Yee et al.¹³ who worked with PMMA/PS blends. Both studies reported a lower (τ_f) for modified blend together with an increase of storage modulus at low frequencies originated from the relaxation of Marangoni stresses induced by a nonuniform distribution of compatibilizers along the surface of the droplet.

The difference between the rheological behavior of the blends to which 1 wt % and to which more than 1 wt % of compatibilizer was added may be explained by the change of capillary number induced by the presence of compatibilizers. The Capillary number [eq. (10)], which is defined as the ratio of hydrodynamic $\eta_m \dot{\gamma}$ and interfacial stresses Γ/R is given by:

$$Ca = \frac{\eta_m \dot{\gamma}}{\Gamma/R} \quad (10)$$

where η_m is the viscosity of the matrix, $\dot{\gamma}$ is the rate of deformation, Γ is the interfacial tension between the components, and R is the radius of the dispersed phase droplets.

As shown eq. (10), the capillary number depends on both the interfacial tension between the components of the blends and the radius of the dispersed phase that are both affected by compatibilizers addition. Table VI presents the particle size reduction ($R_v R$) and interfacial tension reduction (γR) for a given PP-g-PMMA concentration for PMMA/PP blends using the following equations:

$$R_v R = \frac{R_{v0} - R_{vc}}{R_{v0}} \times 100\% \quad (11)$$

$$\Gamma R = \frac{\Gamma_o - \Gamma_c}{\Gamma_o} \times 100\% \quad (12)$$

where R_{v0} and Γ_o are the volume average radius of the dispersed phase of the blend and interfacial tension between PMMA and PP, respectively, without compatibilizer addition, R_{vc} and Γ_c are the volume average radius of the dispersed phase of the blend and interfacial tension between PMMA and PP, respectively, at a given concentration of compatibilizer c .

It can be seen that upon addition of 1 wt % of compatibilizer the reduction of interfacial tension is lower than the one of radius, contrary to what was observed for larger concentrations of

Table VI. Particle Size Reduction (R_vR) and Interfacial Tension Reduction (γR) for a Given PP-g-PMMA Concentration for the Different PMMA/PP Blends

Blend composition	PP-g-PMMA concentration (wt %)	R_vR (%)	γR (%) (Bousmina's Model) ^a
70/30	0	-	-
	1	17	7
	5	34	-
	10	41	64
90/10	0	-	-
	1	17	7
	10	39	64

^aInterfacial tension obtained by fitting the experimental curve of PMMA/PP (90/10) blends and Bousmina's Model.

compatibilizer. The capillary number for the blends to which 1 wt % of compatibilizer was added is therefore smaller than the one of the noncompatibilized blend whereas it is larger for the blends to which a larger concentration of compatibilizer was added. These different values of capillary numbers could explain the faster relaxation for the blends modified with 1 wt % PP-g-PMMA and slower relaxation for the blends modified with larger concentrations of PP-g-PMMA.

The rheological results obtained may also be explained in terms of critical concentration of interface saturation of the compatibilizer. It can be seen from Table VI, that the addition of 1 wt % of PP-g-PMMA to PMMA/PP (70/30) and (90/10) blends resulted in a small dispersed phase reduction and a small interfacial tension between PP and PMMA reduction. Such a behavior could indicate that a concentration of 1 wt % of PP-g-PMMA is below the critical concentration of interface saturation, resulting in a nonhomogenous distribution of the compatibilizer around dispersed droplet surface when submitted to deformation. Such nonhomogenous distribution of the compatibilizer could generate local Marangoni stresses, which normally promote a faster relaxation of the dispersed phase droplets compared with the ones of the blend without compatibilizer addition. Such a behavior has already been observed by Van Puyvelde et al.²³ who studied dispersed phase droplets deformation and relaxation behavior of PDMS/PIB (99/1) blends using a diblock copolymer PIB-PDMS as a compatibilizer and by Mechbal and Bousmina,²⁵ who studied the stress relaxation behavior of 70/30 PMMA/PS (70/30) blends, using a block copolymer PS-*b*-PMMA with blocks having a molar mass above the molecular weight of entanglement. When using this copolymer, Mechbal and Bousmina²⁵ observed a faster relaxation for the blends with a concentration of copolymer below interface saturation. The authors observed that the addition of this type of block copolymer in a concentration below the interface saturation (when the interface was totally recovered by the copolymer) resulted in a high accumulation of the copolymer at the droplet tips. Such copolymer concentration gradient promoted local Marangoni stresses, which resulted in a faster relaxation of the droplets compared to the ones of the blend without block copolymer addition.

CONCLUSIONS

In this work, the morphology and linear viscoelastic behavior of PMMA/PP (70/30 and 90/10) blends to which a graft copolymer PP-g-PMMA was added in concentrations below and above the critical concentration of interface saturation was studied. The following conclusions could be made: PP-g-PMMA is an efficient compatibilizer for PMMA/PP blend as its addition results in a reduction of the size of the PP dispersed phase and in a decrease of interfacial tension between PMMA and PP. The impact of the addition of compatibilizer on the rheological behavior of the blend in the linear viscoelastic regime depends on the compatibilizer concentration. For a concentration of compatibilizer added below the critical concentration of interface saturation (1 wt % PP-g-PMMA), either an increase or decrease of elasticity (storage modulus) at low frequencies can be observed depending on the blend concentration: for low blend concentration, the relaxation of Marangoni stresses induced by the presence of gradient of compatibilizer concentration along the droplet surface can be observed (three relaxation times which can be attributed to the relaxation of individual phases, sheared droplets and Marangoni stresses are observed in the relaxation spectrum) resulting in an increase of storage modulus at low frequencies. For a concentration of compatibilizer added above the critical concentration of interface saturation, an increase of elasticity is observed and only two relaxation times (which can be attributed to the relaxation of individual phases, sheared droplets) are observed in the relaxation spectrum.

ACKNOWLEDGMENTS

The authors would like to thank Brazilian Founding Agencies: Fundação de Amparo à Pesquisa do Estado de São Paulo (FAPESP), Conselho Nacional de Pesquisa e Desenvolvimento (CNPq), and Coordenação de Aperfeiçoamento de Nível Superior (CAPES), for financial support.

REFERENCES

1. Utracki, L. A. *Commercial Polymer Blends*; Chapman & Hall: London, **1998**.
2. Favis, B. D. *Polymer* **1994**, *35*, 1552.
3. Souza, A. M. C.; Demarquette, N. R. *Polymer* **2002**, *43*, 3959.
4. Jeon, H. K.; Zhang, J. B.; Macosko, C. W. *Polymer* **2005**, *46*, 12422.
5. Sundararaj, U.; Macosko, C. W. *Macromolecules* **1995**, *28*, 2647.
6. Garmabi, H.; Demarquette, N. R.; Kamal, M. *Int. Polym. Process* **1998**, *13*, 183.
7. Macaúbas, P. H. P.; Demarquette, N. R. *Polymer* **2001**, *42*, 2543.
8. Brahim, B.; Ait-Kad, A.; Jérôme, R.; Fayt, R. *J. Rheol.* **1991**, *35*, 1069.
9. Graebing, D.; Muller, R.; Palierne, J. F. *Macromolecules* **1993**, *26*, 320.
10. Wu, D.; Zhang, Y.; Yuan, L.; Zhang, M.; Zhou, W. *J. Polym. Sci. Part B: Polym. Phys.* **2010**, *48*, 756.

11. Shi, D.; Hu, G. H.; Ke, Z.; Li, R. K. Y.; Yin, J. *Polymer* **2006**, *47*, 4659.
12. Friederich, C.; Antonov, Y. Y. *Macromolecules* **2007**, *40*, 1283.
13. Yee, M.; Calvão, P.; Demarquette, N. R. *Rheol. Acta.* **2007**, *46*, 653.
14. Huo, Y.; Groeninckx, G.; Moldenaers, P. *Rheol. Acta.* **2007**, *46*, 507.
15. Riemann, R. E.; Cantow, H. J.; Friedrich, C. *Polym. Bull.* **1996**, *36*, 637.
16. Riemann, R. E.; Cantow, H. J.; Friedrich, C. *Macromolecules* **1997**, *18*, 5476.
17. Moan, M.; Huitric, J.; Médéric, P.; Jarrin, J. *J. Rheol.* **2000**, *44*, 1227.
18. Fahrlander, M.; Bruch, M.; Menke, T.; Friedrich, C. *Rheol. Acta.* **2001**, *40*, 1.
19. Velankar, S.; Van Puyvelde, P.; Mewis, J.; Moldenaers, P. *J. Rheol.* **2001**, *45*, 1007.
20. Velankar, S.; Van Puyvelde, P.; Mewis, J.; Moldenaers, P. *J. Rheol.* **2004**, *48*, 725.
21. Van Hemelrijck, E.; Van Puyvelde, P.; Velankar, S.; Macosko, C. W.; Moldenaers, P. *J. Rheol.* **2004**, *48*, 143.
22. Van Hemelrijck, E.; Van Puyvelde, P.; Velankar, S.; Macosko, C. W.; Moldenaers, P. *J. Rheol.* **2005**, *49*, 783.
23. Van Puyvelde, P.; Velankar, S.; Mewis, J.; Moldenaers, P. *Polym. Eng. Sci.* **2002**, *42*, 1956.
24. Iza, M.; Bousmina, M. *J. Rheol.* **2000**, *44*, 1363.
25. Mechbal, N.; Bousmina, M. *Macromolecules* **2007**, *40*, 967.
26. Yee, M.; Souza, A. M. C.; Valera, T. S.; Demarquette, N. R. *Rheol. Acta.* **2009**, *48*, 527.
27. Palierne, J. F. *Rheol. Acta.* **1990**, *29*, 204.
28. Palierne, J. F. *Rheol. Acta.* **1991**, *30*, 497.
29. Bousmina, M. *Rheol. Acta.* **1999**, *38*, 73.
30. Jacobs, U.; Fahrlander, M.; Winterhalter, J.; Friedrich, C. *J. Rheol.* **1999**, *43*, 1495.
31. Underwood, E. E. *Quantitative Sterology*; Addison Wesley: Massachusetts, **1970**.
32. Ares, A.; Silva, J.; Maia, J. M.; Barral, L.; Abad, M. *J. Rheol. Acta.* **2009**, *48*, 993.
33. Ansari, M.; Haghtalab, A.; Semsarzadeh, M. A. *Rheol. Acta.* **2006**, *46*, 983.
34. Honerkamp, J.; Weese, J. *Rheol. Acta.* **1993**, *32*, 65.
35. Calvão, P. S.; Yee, M.; Demarquette, N. R. *Polymer* **2005**, *46*, 2610.
36. Valera, T. S.; Morita, A. T.; Demarquette, N. R. *Macromolecules* **2006**, *39*, 2663.
37. Asthana, H.; Jayaraman, K. *Macromolecules* **1999**, *32*, 3412.
38. Carreau, P. J.; De Kee, D.; Chhabra, R. *Rheology of polymeric systems principles and applications*; Carl Hanser: Munich, Germany, **1997**.
39. Shi, D.; Ke, Z.; Yang, J.; Gao, Y.; Wu, J.; Yin, J. *Macromolecules* **2002**, *35*, 8005.
40. Davies, A. R.; Anderssen, R. S. *J. Non-Newtonian Fluid. Mech.* **1997**, *73*, 163.
41. Macaúbas, P. H. P.; Demarquette, N. R. *Polym. Eng. Sci.* **2002**, *42*, 1509.
42. Shaayegan, V.; Wood-Adams, P.; Demarquette, N. R.; Souza, A. M. C. In *Proceedings of The Polymer Processing Society, 26th Annual Meeting, Banff, Canada, July 4–8, 2010*.